Polymer Bulletin 32, 487–492 (1994)

Polymer Bulletin

Surface morphology of a liquid crystalline side-chain polymer investigated by scanning force microscopy

K. D. Jandt[1,*], D. G. McDonnell[2], J. M. Blackmore[2], and M. J. Miles[1]

[1]H. H. Wills Physics Laboratory, University of Bristol, Royal Fort, Tyndall Avenue, Bristol BS8 1TL, UK
[2]Defence Research Agency, St. Andrews Road, Great Malvern, Worcs WR14 3PS, UK

Summary

Surfaces of a low molecular weight, side-chain liquid crystalline polymer (LCP), slow-cooled from the isotropic melt, have been investigated using the scanning force microscope (SFM) to study its surface morphology. The results obtained from SFM measurements show the hedritic surface morphology of the material. These hedrites, as the assumed precursor state of LCP-spherulites, show diameters between 5 and 10 micrometers. Concentric lamellae of a thickness between 50 and 100 nanometres are the characteristic substructure of the LCP-hedrites. Higher resolution SFM images show a regular fine structure of these lamellae, consisting of band structures organized in domains with a band repeat distance of about 30 nanometres. A great variety of domain boundaries have been obtained.

Introduction

During the last few years the main activities of scanning probe microscopy (SPM) on liquid crystalline materials (LC) have been focused on scanning tunneling microscopy (STM) experiments of alkylated cyanobiphenyls (nCB; n = 6,.., 12) (1-3) or related, low molecular weight materials (4,5) on graphite, MoS_2, WSe_2 or similar compounds. Aims of these investigations were to study the molecular surface arrangement and mesophase states of these materials since they are self organizing and form a stable molecular lattice on the underlying substrate.

Only very few papers have been published about LCs investigated with the scanning force microscopy (SFM) (6,7) owing to experimental difficulties, in particular the weak adhesion of these materials to the underlying substrate. More morphological studies of LCPs have been performed using the transmission electron microscope (TEM) with and without the use of selective etching techniques (see for example (8,9)). These investigations have been carried out owing to a scientific and commercial need to gain the knowledge of morphological characteristics and structures of liquid crystalline materials on a microscopic scale (1 nm to 100 μm), since these molecular superstructures determine many of the LCP physical properties such as fracture toughness and stiffness of fibres. On the other hand, LCP respond to electric and magnetic fields, which makes them suitable for the use in display purposes. An order in the LC state of a polymer caused by an electric or magnetic field can be frozen in by cooling the LCP in its crystalline state (10, 11). This makes LCPs suitable for storage devices.

The SFM is a suitable instrument to image ordered structures in LCPs, since no additional surface coating with carbon or metals, or the use of replica and etching techniques are required. Here we present SFM images of a LCP in the crystalline state showing a distinct three dimensional order. The surface morphology down to the nanometre scale was obtained with the SFM.

*Corresponding author, present address: Dept. of Materials Science and Engineering, Cornell University, Bard Hall, Ithaca, NY 14853-1501, USA

Experimental

After depositing the low molecular weight side-chain liquid crystalline polymer material shown in Fig. 1 (12) onto freshly cleaved mica, the sample was heated to the isotropic state (about 390 K) and spread out on the mica surface, to form a thin liquid film of an estimated thickness of less than 50 µm. Subsequently the sample was slowly cooled down to room temperature at a rate of 0.01 $Kmin^{-1}$. The glass transition temperature T_g of the LCP material is 333 K (13).

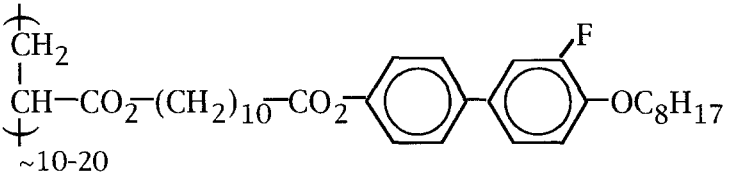

Fig. 1: *Chemical structure of the LCP used for the STM investigations presented here. The molecular length of the extended main chain can vary between 2.6 nm and 5.2 nm. The length of the extended side-chains is about 3.3 nm.*

A Nanoscope III SFM (14) operating at room temperature was used for the investigations. Experiments using the repulsive force mode of operation, where the cantilever tip is in permanent contact with the sample surface, were carried out under propanol (spectrophotometric grade). Propanol was chosen to minimise the capillary forces between the cantilever tip and the surface (15) and because it would not cause the LCP to swell or soften.

The cantilevers used were supplied by the microscope manufacturer, and had a nominal force constant of 0.06 Nm^{-1}. The forces applied with the SFM tip were $\leq 10^{-9}$ N. The imaging force was adjusted to just above the pull-off point of the cantilever as soon as possible after the first contact in order to reduce the applied force to the minimum possible for stable imaging. From time to time it was checked that the set point was stable and still at the same location of the force curve. Image acquisition times ranged from 20 seconds to 1 minute. No filtering was applied to the feedback signal or the images. All Structures shown in the SFM images, were reproducible independent of scanning frequency, scanning direction and x-y range.

Results and Discussion

During the slow cooling process described above, the LCP film crystallises onto the mica surface, forming various three dimensional structures at its surface. This can be seen in the SFM images presented here. As seen in Fig 2 a and b, the LCP has formed distinct surface topography consisting of LCP lamellae. These lamellae are arranged in concentric superstructures similar to hedrites (16). From other polymeric materials hedrites are well known as a precursor state of spherulitic growth (16-18). We interpret the LCP hedrites also as a precursor state of spherulitic growth of the LCP material. The diameter of these hedrites was found to be between 7 µm and 10 µm. Fig. 2 b shows the concentric growth of the lamellae around a common core (nucleus). These growing centres were observed for all hedrites obtained in our investigations. The crystalline growth is believed to start at these cores which may consist of impurities (heterogen crystallisation).

Gradually the lamellae in the hedrites diverge or fan outward in a splaying motion. Repeated splaying, aided by lamellae which are intrinsically curved (see Figs. 2 b and 3 a), may lead to the spherical shape characteristic of a LCP spherulite. The diameter of lamellae building up the hedrites were found to vary between 50 nm and 500 nanometres whereas their length were measured to be several micrometres. The individual lamellae exhibit a variation in thickness, especially at those surface areas, where they change direction (curved lamellae).

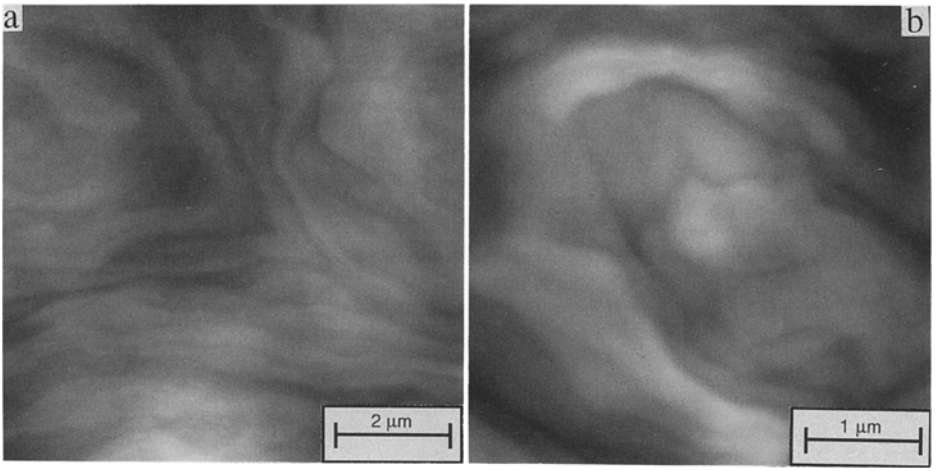

Fig. 2 a, b: *SFM images of a the surface morphology of the LCP. LCP-lamellae are arranged in concentric superstructures similar to so called hedrites. Their diameter was measured to be between 7 µm and 10 µm. Fig. 2 b shows the concentric growth of the lamellae around a common core (nucleus). The crystalline growth is believed to start at these cores which may consist of impurities (heterogen crystallisation).*

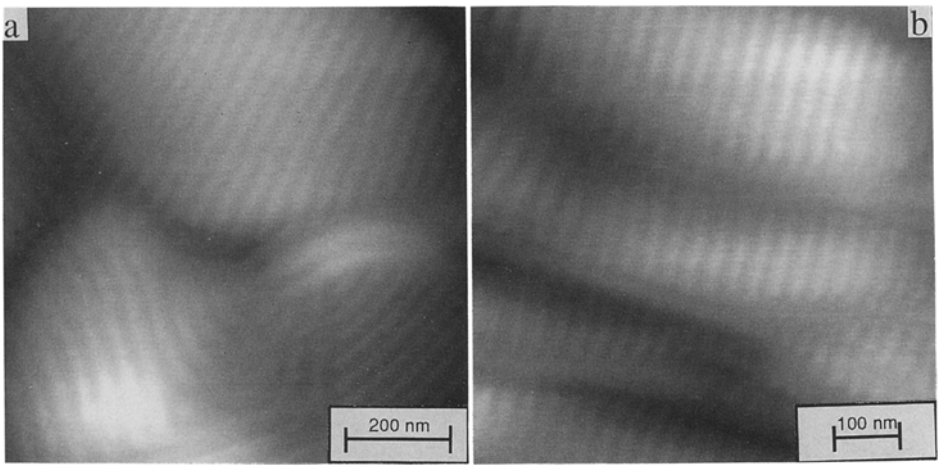

Fig. 3 a, b: *SFM images of the lamellar structures near a hedrite-core region (Fig. 3 a) and at an outer region of the hedrite (Fig 3 b). The diameter of lamellae building up the hedrites were found to vary between 50 nm and 500 nanometres. Note the fine banding structure and its texture within the lamellae. These bands are extended over the full diameter of the lamellae and run perpendicular to the long axes of the lamellae. In this directions, the repeat of the band structures was found to be about 30 nm.*

Fig. 3 a and b show the lamellar surface region near a crystalline growing centre and at an outer region of a hedrite. In these images individual close-packed lamellae can be easily distinguished. The height from the region between the lamellae to the top of the lamellae was measured to be 4 nm ± 2 nm (local values).

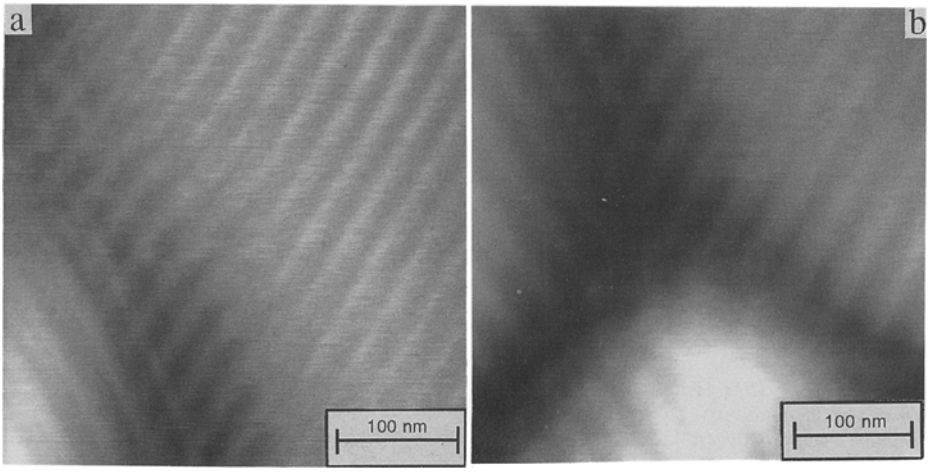

Fig. 4 a, b: *SFM images showing how the bands are organized in different domains. Domain boundaries occur in regions where the lamellae change their growing direction (see Fig. 4 a), or, when some lamellae with different domain orientations meet in a region (Fig. 4 b). In Fig. 4 a two different domain orientations can be seen in one region.*

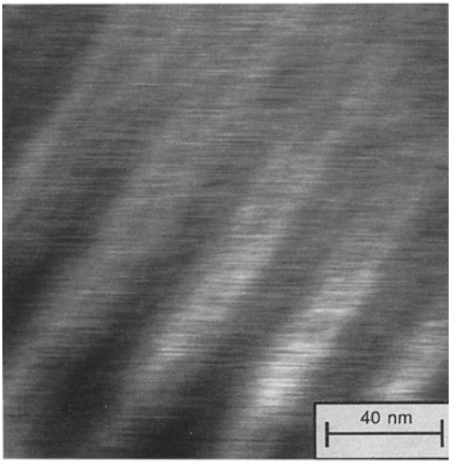

Fig. 5: *SFM image showing individual bands and their substructures. Each bright band of a thickness of about 20 nm consist of two narrow bright bands (diameter of each band rages between 7-8 nm) and one dark region (diameter 6 nm) separate these bands. The difference in height between the bright regions and the dark regions is 0.3 nm ± 0.1 nm.*

Furthermore, the lamellar surfaces exhibits a fine substructure of bands, running approximately perpendicular to the long axes of the lamellae. The length of these bands is always equal to the thickness of the lamella they are part of, since the bands always cross the full diameter of the lamellae. The bands are arranged in domains of various sizes. At the regions where the domains change their direction, a great variety of sharp domain boundaries was obtained. Some examples of these domain boundaries are shown in Fig. 4 a and b.

In general these domain boundaries occur in regions where the lamellae change their growing direction (se Fig. 4 a), or, when some lamellae with different domain orientations meet in a region (Fig. 4 b). In Fig. 4 a two different domain orientations can be seen in one region.

In Fig. 5, the identity period of the bands is about 30 nm can be seen. A detailed analysis of the image shows, that the bands exhibits a substructure. Each bright band of a thickness of about 20 nm consist of two narrow bright subbands (diameter of each subband rages between 7-8 nm) and one dark region (diameter 6 nm) separate these bands. The brightness of these band-substructure corresponds to a difference in height (bright regions higher than dark regions). A height difference of 0.3 nm $\pm$ 0.1 nm was measured between the top of the bright subbands and the bottom of the dark subbands. The fact that a higher, molecular resolution of the LCP surface was not possible, may be presumably due to flexible dangling side- or main chain ends of the LCP at the outermost surface or due to the softness of the sample.

The sizes of the structures in the bands are about the double of the length of the LCP main-chain (between about 2.6 and 5.2 nm) and the side-chain (about 3.3 nm). Therefore the packing of the LCP molecules in the band structure can be understood in terms of a superstructure of the molecular order, e.g., of interdigitating side-chains building up each bright subband. Future X-ray diffraction experiments may help to understand the molecular packing in the banding in more detail.

Conclusions

1. SFM investigations of a low molecular weight, side-chain liquid crystalline polymer (LCP), slow-cooled from the isotropic melt revealed the hedritic surface morphology of the material. These hedrites, build up from concentric lamellae, are the assumed precursor state of LCP-spherulites, with diameters between 5 and 10 micrometers.

2. Higher resolution SFM images show a regular fine structure of these lamellae, consisting of band structures organized in domains with a band repeat distance of about 30 nanometres. A great variety of domain boundaries has been obtained.

3. Within the bands substructures of a few nanometres were obtained. The packing of the LCP molecules in the band structure can be understood in terms of a superstructure of the molecular order, e.g., of interdigitating side-chains building up each bright subband.

Acknowledgement

K. D. Jandt and M. J. Miles gratefully acknowledge the financial support of the SERC. M. J. Miles gratefully acknowledge the financial support of the AFRC.

References

1. Foster JS, Frommer JE (1988) Nature 333: 542
2. Smith DPE, Hörber JK-H, Gerber C, Binnig G (1989) Science 245: 43
3. Hara M, Iwakabe Y, Tochgi K, Sasabe H, Garito A, Yamada A (1990) Nature 344: 228
4. Iwakabe Y, Hara M, Kondo K, Tochigi K, Mukoh A, Yamada A, Garito AF, Sasabe H (1991) Jap. J. Appl. Phys. 30: 2542
5. Sautière L, Day S, Miles MJ (1992) Ultramicroscopy 42-44: 1054

6. Yamada H, Akamine S, Quate CF (1992) Ultramicroscopy 42-44: 1044
7. Terris BD, Twieg RJ, Nguyen C, Sigaud G, Nguyen HT (1992) Europhys. Lett. 19 (2): 85
8. Hudson SD, Lovinger J (1993) Polymer 6: 1123
9. Xu G, Wu W, Shen D, Hou J, Zhang S, Xu M, Zhou Q (1993) Polymer 9: 1818
10. Blinov L M (1983) Electro-optical and Magneto-optical Principals of Liquid Crystals. John Wily and Sons, New York
11. Chandrasekhar S (1992) Liquid Crystals. 2nd Ed. Cambridge University Press, Cambridge
12. The LCP was supplied via the Defence Research Agency, Malvern, England
13. Unpublished data
14. Digital Instruments, Santa Barbara, CA., USA
15. Hansma HG, Vesenka T, Siegenst C, Keldermann G, Momett H, Sinsheimer RL, Eilings V, Bustamante C, Hansma PK (1992) Science 256: 1180
16. Geil PH (1958) in: Doremus RH, Roberts BW, Turnbull D (Eds.) Growth and Perfection of Crystals, Wiley, New York, 579
17. Khoury F, Passaglia E (1976) in: Hannay NB (Ed.) Treatise on Solid State Chemistry, Vol. 3, Crystalline and Noncrystalline Solids, Plenum, New York, Ch. 6
18. Basset DC, Keller A, Mitsuhashi S (1963) J Polym. Sci. A1: 763; Keith, H. D. (1964) J. Polym. Sci. A2: 4339

Accepted January 28, 1994 C